THE JOURNAL OF PHYSICAL CHEMISTRY B

Article

pubs.acs.org/JPCB

Irreversible Catalyst Activation Enables Hyperpolarization and Water Solubility for NMR Signal Amplification by Reversible Exchange

Milton L. Truong,*[,†] Fan Shi,[○] Ping He,[○] Bingxin Yuan,[○] Kyle N. Plunkett,[○] Aaron M. Coffey,[†,‡] Roman V. Shchepin,[†] Danila A. Barskiy,[⊥,#] Kirill V. Kovtunov,[⊥,#] Igor V. Koptyug,[⊥,#] Kevin W. Waddell,[†,§] Boyd M. Goodson,[○] and Eduard Y. Chekmenev*[,†,‡,∥]

[†]Institute of Imaging Science, Department of Radiology, [‡]Department of Biomedical Engineering, [§]Department of Physics and Astronomy, and [∥]Department of Biochemistry, Vanderbilt University, Nashville, Tennessee 37232-2310, United States

[⊥]International Tomography Center, 3A Institutskaya St., Novosibirsk 630090, Russia

[#]Novosibirsk State University, 2 Pirogova St., Novosibirsk 630090, Russia

[○]Department of Chemistry and Biochemistry, Southern Illinois University, Carbondale, Illinois 62901, United States

Supporting Information

ABSTRACT: Activation of a catalyst [IrCl(COD)(IMes)] (IMes = 1,3-bis(2,4,6-trimethylphenyl)imidazol-2-ylidene; COD = cyclooctadiene)] for signal amplification by reversible exchange (SABRE) was monitored by *in situ* hyperpolarized proton NMR at 9.4 T. During the catalyst-activation process, the COD moiety undergoes hydrogenation that leads to its complete removal from the Ir complex. A transient hydride intermediate of the catalyst is observed via its hyperpolarized signatures, which could not be detected using conventional nonhyperpolarized solution NMR. SABRE enhancement of the pyridine substrate can be fully rendered only after removal of the COD moiety; failure to properly activate the catalyst in the presence of sufficient substrate can lead to irreversible deactivation consistent with oligomerization of the catalyst molecules. Following catalyst activation, results from selective RF-saturation studies support the hypothesis that substrate polarization at high field arises from nuclear cross-relaxation with hyperpolarized ^{1}H spins of the hydride/orthohydrogen spin bath. Importantly, the chemical changes that accompanied the catalyst's full activation were also found to endow the catalyst with water solubility, here used to demonstrate SABRE hyperpolarization of nicotinamide in water without the need for any organic cosolvent—paving the way to various biomedical applications of SABRE hyperpolarization methods.

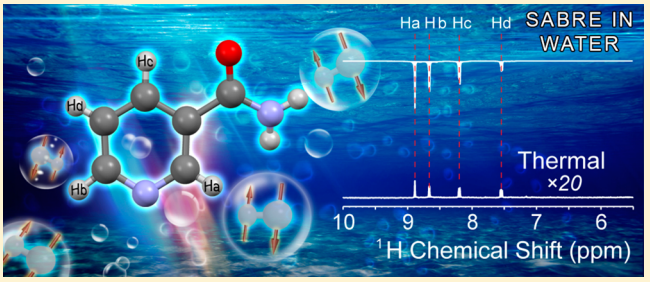

INTRODUCTION

NMR hyperpolarization can temporarily increase nuclear spin polarization by 4−8 orders of magnitude, translating into corresponding increases in NMR and MRI detection sensitivity.[1,2] The sensitivity gains improve the detection limit, which enables new imaging methodologies—including hyperpolarized MRI for molecular imaging of dilute metabolites[3] and functional contrast agents such as hyperpolarized ^{129}Xe.[4,5]

Parahydrogen-based hyperpolarization techniques are special in that they transform the spin order of the parahydrogen gas singlet state into observable nuclear spin polarization (up to order unity) of other molecules. Conventional parahydrogen induced polarization (PHIP)[6] has relied on the molecular addition of parahydrogen to an unsaturated molecular precursor across C═C or C≡C bonds.[7] This technique was further advanced by preserving the high nuclear spin order of nascent parahydrogen pairs on ^{13}C sites with long T_1 relaxation times exceeding 1 min.[8,9] Recent advances in catalysis have also enabled PHIP hyperpolarization of ^{13}C contrast agents in biologically compatible aqueous media in seconds[10,11] with successful application in living organisms.[12−14]

One of the main fundamental limitations of conventional PHIP is the requirement for an unsaturated precursor for molecular addition of parahydrogen (p-H_2). This limitation has been lifted by the introduction of the signal amplification by reversible exchange (SABRE) hyperpolarization technique in 2009.[15,16] As with conventional PHIP, SABRE involves p-H_2 and substrate exchange on metal complexes; however, instead of hydrogenation, hyperpolarization of the substrate molecule is achieved by transfer of spin order originating from p-H_2 during the lifetime of the transient complex.[15−17] Despite the rapid progress of this technique with an expanding list of substrate molecules[18,19] amenable to SABRE and recent demonstration of heterogeneous SABRE (HET-SABRE, where the solubilized substrate exchanges on the metal complex tethered to solid-

Received: October 28, 2014
Revised: November 4, 2014
Published: November 5, 2014

phase support[20]), the chemistry and the mechanism of the SABRE process are still not fully understood. Moreover, despite promising efforts[19,21−24] to mitigate the poor solubility of SABRE catalysts in water, this method has not been demonstrated in pure aqueous media suitable for biomedical applications—the main drivers behind the development of most hyperpolarized magnetic resonance techniques.[25−27]

The work presented here takes advantage of *in situ* high-resolution NMR detection of SABRE at 9.4 T,[28] which unlike low-field *in situ* SABRE detection[17] offers an advantage of exquisite chemical shift dispersion and high-resolution for distinguishing chemical compounds and their sites. Specifically, we demonstrate *in situ* detection of a hyperpolarized intermediate during activation steps of the most potent SABRE catalyst, [IrCl(COD)(IMes)][29,30] (IMes = 1,3-bis-(2,4,6-trimethyl-phenyl)imidazol-2-ylidene; COD = cyclooctadiene). It is found that the SABRE effect is activated only when the COD moiety is removed via its hydrogenation to cyclooctene and cyclooctane in agreement with previous studies.[31] Furthermore, such activation requires the presence of excess substrate in order to avoid side reactions that irreversibly deactivate the catalyst (likely involving catalyst oligomerization). *In situ* studies of high-field SABRE with the activated catalyst are consistent with substrate enhancements resulting from cross-relaxation with hyperpolarized hydride spins in a manner akin to the spin-polarization induced nuclear Overhauser effect (SPINOE).[28,42] Finally, because of the catalyst's chemical changes that occur during activation, it is possible to solubilize the activated catalyst in aqueous media, which previously has not been demonstrated without the use of organic cosolvents.[19,22] SABRE hyperpolarization of nicotinamide (the amide of vitamin B_3) in water is shown as a proof of principle for potential biological applications.

EXPERIMENTAL SECTION

All solutions were placed in 9 in. long, 5 mm medium-wall (0.77 mm-thick) NMR tubes. The end of the NMR tube (~3/4 in. long) was placed inside a piece of Teflon tubing (~2 in. long, 1/4 in. OD, 3/64 in. wall thickness) to provide high-pressure connection to a wye (for "Y" shape connection) 0.25 in. push-to-connect fitting (McMaster Carr, P/N 5779K44) (Figure 1). The top two ends of the wye fitting were connected to ~1 in. long pieces of the same 0.25 in. OD Teflon tubing. On one end, a push-to-connect reducing connector (McMaster Carr, P/N 5779K352) was used to connect a 0.125 in. OD Teflon tubing line to provide an exhaust path for "used" p-H_2 gas exiting the solution. On the other top end, connectors (McMaster Carr, P/N 9087K121 and Western Analytical, P/N U-510−01) were used to allow 0.125 in. OD (1/16 in. ID) tubing, connected via a short flangeless nut (Western Analytical, P/N XP-208X), to extend all the way through the length of 5 mm NMR tube to reach to the bottom of 5 mm NMR tube to deliver fresh p-H_2 gas to the bottom of NMR tube for efficient bubbling through the entire content of the NMR tube. High-pressure experiments were conducted by attaching a safety valve (one-way, calibrated to the exact pressure rating) to the exhaust gas line to allow p-H_2 pressure of up to 5.1 bar. All NMR experiments were conducted using a 9.4 T (400 MHz) Bruker Avance III spectrometer.

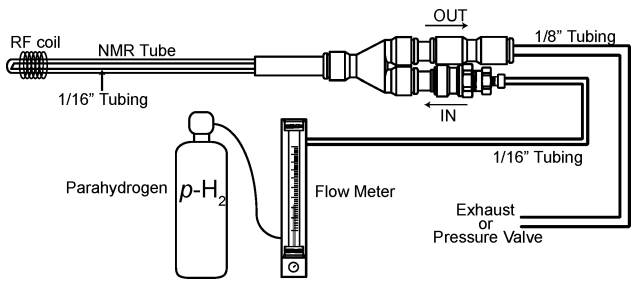

Figure 1. Experimental setup for SABRE with controlled parahydrogen (p-H_2) bubbling through a catalytic solution in a 5 mm NMR tube. The solution sits in a medium-wall NMR tube where p-H_2 is delivered via 1/16 in. OD Teflon tubing. A wye push-to-connect adapter allows parahydrogen to flow into the NMR tube, while allowing for the expended gas to leave the detection volume via the exhaust line. The exhaust line can be capped with a pressure-calibrated safety valve to conduct SABRE at a higher p-H_2 pressure.

The iridium [IrCl(COD)(IMes)][30] (Ir-IMes) catalyst was synthesized as described previously.[28,30] All SABRE studies of pyridine (Py) at high magnetic field were conducted with the Ir-IMes catalyst dissolved in either methanol-d_4, ethanol-d_6, or deuterated water. For the methanol-d_4-based solutions, the complex consisted of 8 mM Ir-Imes and 47 mM Py in 1 mL of methanol-d_4. The ethanol-d_6-based solutions contained 8 mM Ir-IMes and 32 mM Py in 1 mL of ethanol-d_6. All NMR experiments with Py were performed as high-field SABRE[28] experiments wherein p-H_2 was bubbled through the solution and NMR detection was performed at 9.4 T. For *in situ* high-field SABRE detection with Py, the NMR tube was placed into the magnet similar to a typical solution NMR experiment. P-H_2 gas (>90% para-state prepared using previously described instrumentation[32]) was bubbled through a given solution at a flow rate of 0.7 mL/s under atmospheric pressure for durations ranging from 30 to 60 s, depending upon the experiment. ^{1}H NMR spectra were acquired immediately (3 ± 2 s) after the bubbling was stopped.

Experiments with nicotinamide utilized a solution of 3.5 mM Ir-IMes combined with 35 mM nicotinamide in 0.7 mL of ethanol-d_6, D_2O, or a mixture of both. Solutions of 33% and 50% D_2O in ethanol-d_6 were obtained by diluting the activated Ir-Imes/nicotinamide solution in ethanol-d_6 (~0.7 mL volume) with either one or two aliquots of D_2O (~0.35 mL each), respectively. All SABRE experiments with nicotinamide were conventional (low-field) SABRE,[15,16] where p-H_2 was bubbled in the fringe field of the 9.4 T magnet (the solution in the NMR tube experienced 6 ± 4 mT SABRE polarization field; this field strength was measured using a portable gauss meter). Once p-H_2 bubbling was stopped, the sample was quickly transferred inside a 9.4 T NMR magnet for ^{1}H spectra acquisition with only a 5 ± 2 s delay between the end of p-H_2 bubbling and the beginning of the NMR spectra acquisition. During activation, p-H_2 bubbling was performed under atmospheric pressure with a flow rate of 0.7 mL/s. Once the nicotinamide solution was fully activated, p-H_2 bubbling occurred under 5.1 bar of pressure with a flow rate of 1.2 mL/s.

All experiments were conducted at room temperature (~300 K). The experiments conducted *in situ* (within an 9.4 T NMR magnet) utilized no active temperature control, with the room-temperature air supply providing temperature stabilization.

RESULTS AND DISCUSSION

Activation of Ir-IMes-Py with p-H_2. The SABRE activation of Ir-IMes with pyridine (Py) in methanol-d_4 was investigated using high-resolution ^{1}H NMR spectroscopy at 9.4

dx.doi.org/10.1021/jp510825b | J. Phys. Chem. B 2014, 118, 13882−13889

T (Figure 2). The spectrum of the nonactivated catalytic Ir complex (Figure 2a) clearly displays the ^{1}H chemical shift

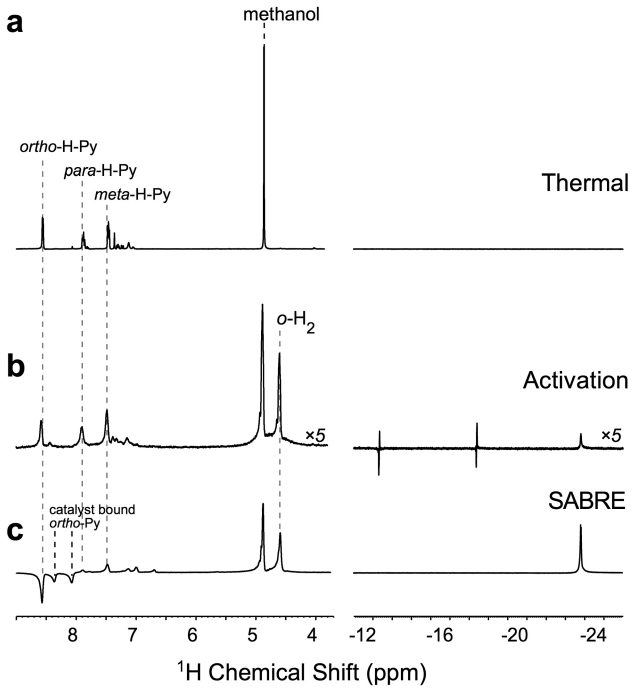

Figure 2. Series of ^{1}H NMR spectra illustrating the hyperpolarization of the Ir-IMes-Py complex in methanol-d_4 by high-field SABRE at 9.4 T.[28] (a) Thermally polarized spectrum of the catalytic complex and Py before p-H_2 is introduced to initiate high-field SABRE. (b) Spectrum recorded immediately after the introduction of p-H_2 (first point in Figure 3c) to the catalyst/Py solution. Note the dispersive peaks from the intermediate hydride species at −12.3 ppm and −17.4 ppm. (c) Spectrum of the Ir-IMes-Py reaction mixture after the catalyst has been completely activated through p-H_2 bubbling. Note that only one hydride species is seen, manifested by an absorptive peak at −22.8 ppm. Additionally, the selective high-field SABRE[28] hyperpolarization of *ortho*-H-Py protons is apparent with the opposite phase of these proton peaks.

signatures of the *ortho*-, *meta*-, and *para*-protons of Py, and the methanol solvent (4.8 ppm). Upon hydrogenation by p-H_2 bubbling (Figure 2b), the formation of three resonances (at −12.3, −17.4, and −22.8 ppm) from hyperpolarized hydride species are observed, in addition to that from hyperpolarized orthohydrogen (o-H_2)[28] at 4.5 ppm. During catalyst activation the high-field SABRE signal of Py was monitored *in situ*. As the catalyst is subjected to additional p-H_2 bubbling, the hydride intermediate is quickly depleted, leaving a single hyperpolarized hydride signal at −22.8 ppm (Figure 2c).[16,28] Once the Ir-IMes-Py complex is fully activated, high-field SABRE signal enhancement is observed on the *ortho*-protons of pyridine (manifested by the large "negative" or emissive signals), o-H_2 (manifested by "positive" or absorptive enhanced signals), and the hydride peaks. Therefore, the introduction of p-H_2 to the catalyst solution initiates the hydrogenation of the COD moiety followed by its complete removal as detected here by high-field SABRE. This conclusion is further supported by the disappearance of COD proton NMR resonances in the spectra of the activated catalyst producing SABRE effect (Figures S1a, S1c-d, and 1d in ref 28) A single intermediate hyperpolarized hydride species (seen as NMR resonances at −12.3 and −17.4 ppm) is likely to be short-lived (both chemically and hyperpolarization-wise with low ^{1}H T_1) and would be difficult to detect by performing the conventional SABRE hyperpolarization procedure in low magnetic field followed by sample transfer to the high magnetic field in a high-resolution NMR spectrometer (as well as by conventional NMR without p-H_2). Indeed, Figure 3b shows that after ∼12 min of p-H_2

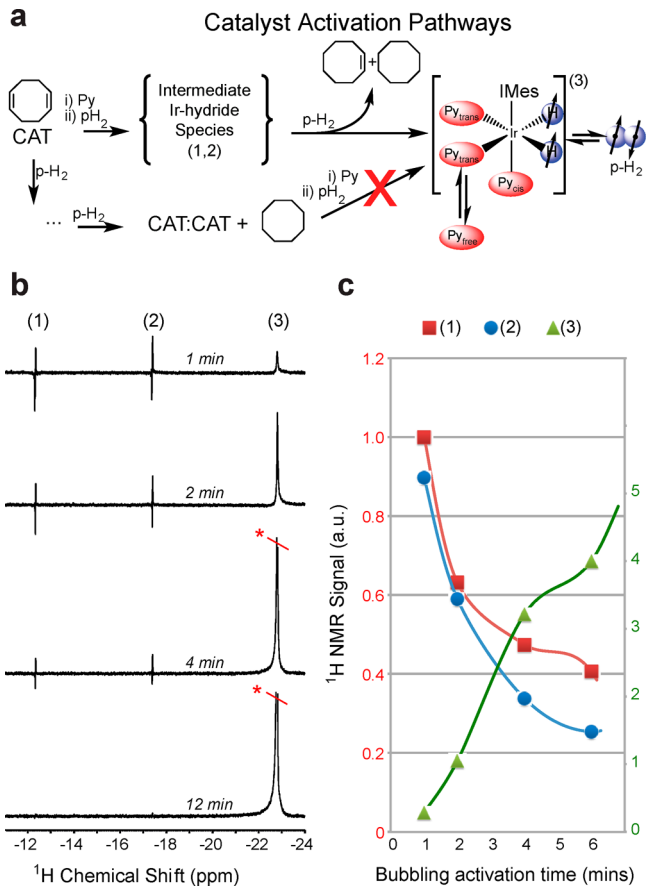

Figure 3. (a) Schematic showing the tentative mechanisms underlying activation and SABRE hyperpolarization with IMes-Ir catalyst and Py. The hydrogenation of COD containing catalyst forms intermediate species corresponding to transient NMR resonances (**1**) and (**2**), before forming the hyperpolarized catalyst-pyridine complex corresponding to NMR resonance (**3**). Additionally, without the presence of pyridine, the activation mechanism reverts to forming an inactive species, possibly a catalyst dimer (CAT:CAT)/oligomer, see Supporting Information) that does not hyperpolarize via SABRE. (b) NMR spectra demonstrating transient dispersive NMR resonances (**1** and **2**) of intermediate hydride species during the activation process. (c) Plot showing the decay (measured as the integrated NMR signal in magnitude mode) of the transient NMR resonances (**1** and **2**)] and the rise of hyperpolarized Ir−hydride resonance (**3**) at −22.8 ppm corresponding to the activated catalyst. The trend lines are added to guide the eye.

bubbling, all signatures of the hyperpolarized hydride intermediate species are absent from the ^{1}H NMR spectrum. The hyperpolarized intermediate hydride species is likely the result of p-H_2 pair being added in the axial and equatorial positions (vs both p-H_2 exchanging in equatorial position only as shown in structure **3**, Figure 3a, of the fully activated Ir−catalyst complex). This observation is in agreement with pioneering work by Bowers and Weitekamp,[33] who detected similar dispersive signatures with Wilkinson's catalyst after

dx.doi.org/10.1021/jp510825b | J. Phys. Chem. B 2014, 118, 13882−13889

addition of p-H_2 in equatorial and axial positions of hexacoordinate Rh(I) complex with similar geometry. Moreover, the phase of these dispersive resonances uniquely reports on the sign of homonuclear J-coupling between two hydride protons in this intermediate species, and it is negative.[33]

It should be pointed out that the high-field SABRE of Py *ortho*-protons effect correlates well with formation of hyperpolarized hydride at −22.8 ppm (estimated qualitatively through correlation of peak intensities of SABRE enhancement of *ortho*-H-Py peak with the rise of the Ir−dihydride peak), likely indicating that this species is responsible for the high-field SABRE effect. The proposed mechanism for catalyst activation/formation[16] is shown in Figure 3a, where the catalyst proceeds through hydrogenation steps (intermediate Ir−hydride species corresponding to transient NMR resonances **1** and **2**) before the fully activated species (**3**) is formed to yield high-field SABRE hyperpolarization of Py. Additional evidence is provided by detection of cyclooctane/cyclooctene vs cyclooctadiene in the ^{1}H NMR spectra[28] before and after full catalyst activation, respectively (data not shown). The *in situ* high-field SABRE may also be a potentially useful tool for studies related to identification and discrimination of classical and nonclassical hydrides in the context of SABRE.[34] We also note that while the enhancements of *in situ* high-field SABRE described here and previously[28] are relatively small, much larger enhancements can be observed with the application of appropriate pulse sequences.[35,36]

The proper activation of Ir-IMes requires not only H_2, but also the presence of sufficient substrate to form a fully coordinated Ir−hydride complex with SABRE properties.[16] In the absence of the ligating substrate (Py), addition of H_2 to the Ir-IMes catalyst likely results in (i) COD removal via hydrogenation and (ii) irreversible formation of inactive species (potentially dimer or trimer species). Our attempts to observe SABRE hyperpolarization with such catalyst states were unsuccessful—even with subsequent additions of Py and p-H_2. Additional evidence of possible dimer/trimer formation is provided in the Supporting Information. The potential oligomerization would be in agreement with previous observation of dimer formation of Crabtree's catalyst[37] (similar to the Ir-IMes catalyst used here) as well as observation of oligomerization in catalysts from the same family.[38] From the perspective of practical consideration, deactivation of this catalyst occurs when the substrate (Py or others) is either absent or present in insufficient concentrations, yielding a solution that remains yellow at the concentrations studied, while the properly activated system turns clear upon complete activation.

NMR Radio Frequency (RF) Saturation Studies. In the high-field SABRE effect, hyperpolarization occurred within the 9.4 T field of the high-resolution NMR spectrometer, and the following signal enhancements occur: Ir−hydride (at −22.8 ppm) and o-H_2 (both with absorptive signals), and the selective (emissive) enhancement of the *ortho*-protons of pyridine (*ortho*-H-Py) in free and catalyst-bound forms, Figure 2c.[28] Here, the activated catalytic complex (**3**) was further probed to study chemical and polarization exchange in three hyperpolarized species by applying frequency selective RF irradiation during p-H_2 bubbling (i.e., RF irradiation was applied throughout the entire 60 s-long bubbling step) during the build-up phase of the high-field SABRE effect. Application of a frequency-selective saturation RF pulse at the hyperpolarized hydride resonance frequency during SABRE polarization (Figure 4a) revealed that the hyperpolarized o-H_2 signal (at 4.5 ppm) was suppressed along with the hydride signal (at

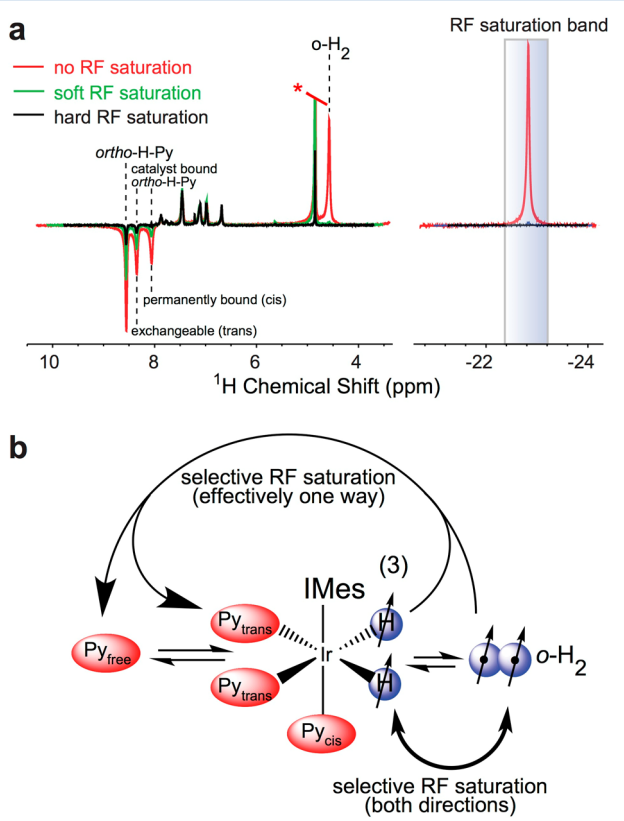

Figure 4. High-resolution proton NMR RF-saturation study via *in situ* detection of high-field SABRE. (a) NMR spectra were recorded 3 ± 2 s after p-H_2 bubbling was stopped inside the 9.4 T magnet of the NMR spectrometer. The color-coded NMR spectra were recorded under conditions of variable RF-power saturation ("soft" (green trace) with $B_1 \sim 7.5$ Hz; "hard" (black trace) with $B_1 \sim 2.4 \times 10^2$ Hz; and "no" (red trace) RF saturation pulses) applied at the Ir−hydride resonance frequency during *in situ* p-H_2 bubbling. Continuous RF irradiation on the hydride peak diminishes the polarization enhancements at both the o-H_2 peak (4.5 ppm), and the *ortho*-H-Py peaks (8.05−8.55 ppm) in addition to destroying the hydride hyperpolarized signal. The same trend is observed for RF-saturation at o-H_2 (see Supporting Information) as depicted in the scheme shown in part b. However, RF saturation on the *ortho*-H-Py has little observable effect on the polarization of Ir−hydride and o-H_2 (see Supporting Information). Frequency-selective RF saturation was applied during high-field SABRE hyperpolarization (p-H_2 bubbling for 60 s at 9.4 T).

−22.8 ppm) even with very soft ($B_1 \sim 7.5$ Hz) RF saturation. Importantly, the *ortho*-H-Py hyperpolarized signal intensities were suppressed such that the high-field SABRE enhancements were significantly reduced under conditions of a relatively strong ($B_1 \sim 2.4 \times 10^2$ Hz) RF saturation on the hydride spectral band (Figure 4a, black trace). When RF saturation is applied at the o-H_2 frequency (Figure S1, Supporting Information), a similar trend is observed, with nearly full depletion of the hyperpolarized Ir−hydride peak, and partial depletion of *ortho*-H-Py peaks as in Figure 4a, black trace. Shifting the RF saturation to the *ortho*-H-Py (corresponding to free Py in solution, ^{1}H resonance at ∼8.55 ppm) resonances leads to a different trend (Figure S1c, where only the *ortho*-H-Py resonances of free Py and exchangeable Py (∼8.33 ppm) are clearly suppressed. RF saturation of free *ortho*-H-Py has little

dx.doi.org/10.1021/jp510825b | J. Phys. Chem. B 2014, 118, 13882−13889

observable effect on the hyperpolarization enhancements for *ortho*-H_2, Ir−hydride, and catalyst-bound (nonexchangeable in cis- position) *ortho*-H-Py.

The one-H-PHIP[39] mechanism is a potential candidate to explain the current and previous[28] observation of high-field SABRE effect, when at least one of the hydrogen atoms from *p*-H_2 molecule is incorporated via hydrogen exchange. However, while such exchange is indeed present, and is concurrent with the SABRE processes, it occurs on a much longer time scale of days and therefore cannot explain high- or low-field SABRE effects.[28]

On the basis of the RF saturation experimental results described above the following high-field SABRE model is proposed (Figure 4b). Hyperpolarization of exchangeable and free *ortho*-H-Py (the residence time of exchangeable Py sites is on the order of 0.1−0.2 s[40]) is induced by the hyperpolarization pool of *o*-H_2 and Ir−hydride, but not the other way around. This model is in agreement with previously proposed spin polarization-induced nuclear Overhauser effect (SPI-NOE):[4,28,41,42] The catalyst's interaction with *p*-H_2 produces high *z*-magnetization in the form of hyperpolarized hydride and *o*-H_2. The close proximity of hyperpolarized hydride spins then drives the bound *ortho*-H-Py spins out of thermal equilibrium via nuclear dipolar cross-relaxation (which then results in enhanced spectra of free *ortho*-H-Py as well; note that emissive enhancements would be consistent with expectation that the double-quantum term of the NOE should dominate in the extreme-narrowing regime). On the other hand, reduction or destruction of the hydride/*o*-H_2 z-magnetization suppresses the high-field SABRE enhancement—consistent with the conclusion that *p*-H_2 itself is not the *direct* source of spin order for high-field SABRE.

Water-Soluble SABRE Catalytic Complex. Prior to activation, the Ir-IMes catalyst (with its COD ligand intact) is insoluble in water, even with the presence of SABRE substrates such as Py or nicotinamide added to the solution. Therefore, organic solvents such as methanol-d_4, ethanol-d_6 or DMSO are typically used to solubilize the Ir-IMes catalyst for SABRE hyperpolarization.[18] However, it was found that when the activated, hexacoordinate Ir-IMes complex generated in methanol or ethanol is dried, the resulting activated complex could be dissolved in pure water. This highly desirable characteristic is likely endowed by the chemical changes that accompany catalyst activation, including the loss of the hydrophobic COD moiety.

Motivated by the biomedical utility of hyperpolarization techniques, SABRE hyperpolarization of nicotinamide in aqueous media was tested owing to the molecule's biological relevance (it belongs to the vitamin B group). Here, Ir-IMes was activated with nicotinamide in ethanol-d_6, achieving hyperpolarization on the four aromatic protons located on the pyridine ring via SABRE at 6 ± 4 mT detected at 9.4 T (Figure 5a). The SABRE polarization enhancements for free nicotinamide protons approach $\varepsilon \sim 100$ and are shown in Table 1. Two sequential aliquots of D_2O were added that resulted in reductions of SABRE hyperpolarization enhancements (Table 1) for all protons except for Hd, which exhibited low polarization enhancements. A separately prepared (after full activation with H_2 in ethanol) catalyst/nicotinamide sample was dried and then reconstituted in pure D_2O. The structure of this complex is expected to be similar to that described by Cowley and co-workers for this catalyst and pyridine.[29] SABRE polarization enhancements approaching $\varepsilon \sim 30$ were observed

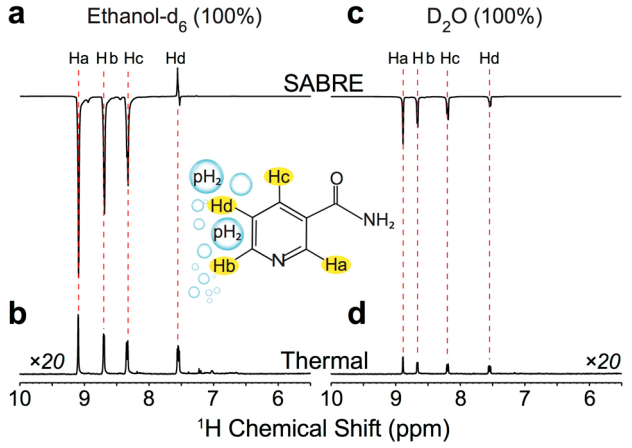

Figure 5. Conventional (low-field) SABRE hyperpolarization of nicotinamide in ethanol-d_6 (a) and in D_2O (c) yields signal enhancement of four aromatic proton peaks of interest (Ha, Hb, Hc, and Hd), with the position of each proton labeled in the structure inset. The enhancement (ε) values for SABRE polarization of nicotinamide using the Ir-IMes catalyst can be found in Table 1. The respective thermally polarized reference ^{1}H NMR spectra of nicotinamide in ethanol-d_6 and D_2O are shown in parts b and d; these thermal spectra are magnified by 20-fold relative to the corresponding hyperpolarized spectra. Note that the apparent "lower" peak heights in thermal spectrum of aqueous sample vs thermal spectrum of the sample in ethanol-d_6 is likely the result of partial sample reconstitution from the dried solid into aqueous medium. Note that SABRE was conducted conventionally at low field (6 ± 4 mT), and it was detected by high-resolution proton NMR spectroscopy (at 9.4 T) using the activated Ir-IMes catalyst in ethanol-d_6 and D_2O.

for most nicotinamide aromatic proton peaks in 100% D_2O (Figure 5c). The preparation procedure for the solution corresponding to the spectrum shown in Figure 5c was different from those reported earlier by Zeng and co-workers,[22] Mewis and coworkers,[24] and Hövener and co-workers[19] in that once the SABRE catalyst activation is achieved in ethanol, the activated complex solution is dried on a rotovap first, and the catalyst/nicotinamide mixture is then reconstituted in 100% D_2O. This approach offers multiple advantages. First, the water-insoluble COD and its hydrogenation products do not migrate into the aqueous phase. Moreover, the use of 10% alcohol in previous works[19] prevents potential *in vivo* injections, while 100% D_2O solutions prepared using the method described here potentially allows for *in vivo* use of SABRE hyperpolarized contrast agents via intravenous administration.

The smaller polarization enhancements achieved in D_2O versus the organic solvents can be largely attributed to the reduced solubility of hydrogen gas in water. Previous studies have shown that H_2 is up to 14 times more soluble by molar fraction in organic solvents than in water.[43−45] The reduced solubility of H_2 in aqueous media limited the effectiveness of *p*-H_2 bubbling in our setup and hindered the ability of *p*-H_2 to interact with the catalytic Ir complex needed for SABRE to occur. However, potential solutions such as increasing the partial *p*-H_2 pressure may recover the enhancement reduction in water versus that observed in ethanol. Moreover, the decrease in the SABRE signal enhancements in water vs ethanol may be also caused by the difference in T_1 relaxation times, which can be lower in aqueous media compared to that in organic solvent media.

dx.doi.org/10.1021/jp510825b | J. Phys. Chem. B 2014, 118, 13882−13889

Table 1. Polarization Enhancement Values (ε) for Four Aromatic Protons of Nicotinamide (Figure 5) Achieved via Conventional (Low-Field) SABRE and Detected by High-Resolution Proton NMR Spectroscopy Using the Activated Ir-IMes Catalyst in Ethanol-d_6, D_2O, and Their Mixtures[a]

medium	ε(Ha)	ε(Hb)	ε(Hc)	ε(Hd)
ethanol-d_6 (100%)	−88.1 ± 0.3	−71.2 ± 0.8	−64.7 ± 2.9	9.1 ± 0.1
ethanol-d_6 (50%), D_2O (50%)	−74.1 ± 11.5	−54.8 ± 4.3	−40.0 ± 0.9	9.3 ± 0.4
ethanol-d_6 (33%), D_2O (67%)	−56.3 ± 4.7	−42.6 ± 0.2	−33.3 ± 4.1	10.0 ± 0.6
D_2O (100%)	−33.3 ± 6.1	−29.5 ± 1.8	−24.0 ± 1.2	−11.0 ± 0.4

[a]SABRE hyperpolarization was conducted at 6 ± 4 mT and detected at 9.4 T.

Furthermore, the low-field SABRE proton signal enhancements for nicotinamide in ethanol were significantly lower than SABRE enhancements reported by other groups, when using more advanced specialized SABRE equipment.[18,29] The experimental limitations (including the lack of precise field control, introduction of p-H_2 via bubbling and potentially longer NMR sample shuttling time) resulted in significantly reduced SABRE signal enhancements in the presented study. Therefore, the reported enhancements for nicotinamide in water can be potentially significantly improved using more advanced hyperpolarization hardware as well the optimization of temperature[18] and p-H_2 pressure, because these experimental variables are related to nicotinamide residency/SABRE contact time on this Ir-dihydride complex.

CONCLUSIONS

The activation and mechanism for hyperpolarization of the Ir-IMes catalyst in alcoholic and aqueous media was probed using *in situ* high-field SABRE.[28] Introduction of p-H_2 to the catalyst in the presence of pyridine substrate initiates a hydrogenation of the COD moiety, leading to intermediate species. SABRE hyperpolarization of the activated catalytic complex results in the enhancement of Ir−hydride, o-H_2, and *ortho*-H-Py protons in free and catalyst-bound forms. RF saturation studies probing polarization and chemical exchange of the hyperpolarized species support the conclusion that substrate hyperpolarization at high field (9.4 T)[28] arises from cross-relaxation with protons belonging to the hyperpolarized hydride/o-H_2 spin bath.

Once activated and dried, the Ir-IMes catalyst was found to be soluble in aqueous media with either Py and nicotinamide substrates incorporated into its hexacoordinate structure. SABRE of nicotinamide substrate in D_2O was conducted using conventional low-field SABRE[15,16,46] and detected at 9.4 T. The SABRE enhancements achieved in aqueous media, while significant ($\varepsilon \sim 30$), were somewhat smaller than those in ethanol-d_6 (Table 1)—which likely reflects the lower solubility of hydrogen gas in water versus ethanol.[19,45] Nevertheless, the SABRE enhancements in water can be potentially increased through the use of higher p-H_2 partial pressures (e.g., ≥10 bar) frequently used in conventional PHIP.[10] Furthermore, additional gains of aqueous SABRE enhancements may be realized through better mixing of catalyst/substrate solution with p-H_2, which has already been shown through the use of solution spray injection in p-H_2 atmosphere,[47,48] or hollow fiber membranes,[23,49] and the optimization of other conditions (e.g., temperature and magnetic field).[18,24]

In any case, the ability to conduct SABRE hyperpolarization with biologically relevant molecules in aqueous media significantly increases the value of SABRE to generate hyperpolarized contrast agents for *in vivo* molecular imaging—eliminating one of the major shortcomings of the SABRE hyperpolarization method. Furthermore, other substrates beyond those studied here can be potentially hyperpolarized in aqueous media, including recently reported tuberculosis drugs pyrazinamide and isoniazid.[18] Finally, it may be possible to combine aqueous SABRE hyperpolarization with HET-SABRE,[20] potentially allowing the preparation of pure aqueous hyperpolarized contrast agents with a recyclable catalyst. The latter can potentially enable not only clinical translation of this hyperpolarization technique, but also high-speed and high-throughput production of hyperpolarized contrast agents at relatively low cost.

ASSOCIATED CONTENT

Supporting Information

Additional figures and tables providing quantitative measurements of RF saturation transfer in NMR experiments and the experimental evidence for catalyst dimer formation. This material is available free of charge via the Internet at http://pubs.acs.org.

AUTHOR INFORMATION

Corresponding Authors

*(M.L.T.) Correspondence address: Department of Radiology, Vanderbilt University Institute of Imaging Science, Nashville, TN 37232. E-mail: milton.truong@vanderbilt.edu.

*(E.Y.C.): Correspondence address: Department of Radiology, Vanderbilt University Institute of Imaging Science, Nashville, TN 37232. Telephone: (615) 322-1329. Fax: (615) 322-0734. E-mail: eduard.chekmenev@vanderbilt.edu.

Author Contributions

All authors have given approval to the final version of the manuscript.

Notes

The authors declare no competing financial interest.

ACKNOWLEDGMENTS

This work was supported by the RAS (5.1.1), RFBR (14-03-00374-a, 14-03-31239-mol-a, 12-03-00403-a, 14-03-93183 MCX_a), SB RAS (57, 60, 61, 122), and the Council on Grants of the President of the Russian Federation (MK-4391.2013.3). We thank for funding support NIH 5R00 CA134749-03, 3R00CA134749-02S1, DoD CDMRP Breast Cancer Program Era of Hope Award W81XWH-12-1-0159/BC112431, NSF CHE-1416268, and NIH 1R21EB018014-01A1. We thank Dr. Panayiotis Nikolaou for professional support with artwork preparation.

REFERENCES

(1) Ardenkjaer-Larsen, J. H.; Fridlund, B.; Gram, A.; Hansson, G.; Hansson, L.; Lerche, M. H.; Servin, R.; Thaning, M.; Golman, K. Increase in Signal-to-Noise Ratio of > 10,000 Times in Liquid-State NMR. *Proc. Natl. Acad. Sci. U.S.A.* **2003**, *100*, 10158−10163.

(2) Nikolaou, P.; Coffey, A. M.; Barlow, M. J.; Rosen, M.; Goodson, B. M.; Chekmenev, E. Y. Temperature-Ramped ^{129}Xe Spin Exchange Optical Pumping. *Anal. Chem.* **2014**, *86*, 8206−8212.
(3) Kurhanewicz, J.; Vigneron, D. B.; Brindle, K.; Chekmenev, E. Y.; Comment, A.; Cunningham, C. H.; DeBerardinis, R. J.; Green, G. G.; Leach, M. O.; Rajan, S. S.; et al. Analysis of Cancer Metabolism by Imaging Hyperpolarized Nuclei: Prospects for Translation to Clinical Research. *Neoplasia* **2011**, *13*, 81−97.
(4) Goodson, B. M. Nuclear Magnetic Resonance of Laser-Polarized Noble Gases in Molecules, Materials, and Organisms. *J. Magn. Reson.* **2002**, *155*, 157−216.
(5) Schroder, L. Xenon for NMR Biosensing - Inert but Alert. *Phys. Med.* **2013**, *29*, 3−16.
(6) Eisenschmid, T. C.; Kirss, R. U.; Deutsch, P. P.; Hommeltoft, S. I.; Eisenberg, R.; Bargon, J.; Lawler, R. G.; Balch, A. L. Para Hydrogen Induced Polarization in Hydrogenation Reactions. *J. Am. Chem. Soc.* **1987**, *109*, 8089−8091.
(7) Bowers, C. R.; Weitekamp, D. P. Transformation of Symmetrization Order to Nuclear-Spin Magnetization by Chemical-Reaction and Nuclear-Magnetic-Resonance. *Phys. Rev. Lett.* **1986**, *57*, 2645−2648.
(8) Goldman, M.; Johannesson, H. Conversion of a Proton Pair Para Order into C-13 Polarization by Rf Irradiation, for Use in MRI. *C. R. Phys.* **2005**, *6*, 575−581.
(9) Cai, C.; Coffey, A. M.; Shchepin, R. V.; Chekmenev, E. Y.; Waddell, K. W. Efficient Transformation of Parahydrogen Spin Order into Heteronuclear Magnetization. *J. Phys. Chem. B* **2013**, *117*, 1219−1224.
(10) Chekmenev, E. Y.; Hovener, J.; Norton, V. A.; Harris, K.; Batchelder, L. S.; Bhattacharya, P.; Ross, B. D.; Weitekamp, D. P. PASADENA Hyperpolarization of Succinic Acid for MRI and NMR Spectroscopy. *J. Am. Chem. Soc.* **2008**, *130*, 4212−4213.
(11) Shchepin, R. V.; Coffey, A. M.; Waddell, K. W.; Chekmenev, E. Y. Parahydrogen Induced Polarization of 1-^{13}C-Phospholactate-D2 for Biomedical Imaging with >30,000,000-Fold NMR Signal Enhancement in Water. *Anal. Chem.* **2014**, *86*, 5601−5605.
(12) Bhattacharya, P.; Chekmenev, E. Y.; Perman, W. H.; Harris, K. C.; Lin, A. P.; Norton, V. A.; Tan, C. T.; Ross, B. D.; Weitekamp, D. P. Towards Hyperpolarized ^{13}C-Succinate Imaging of Brain Cancer. *J. Magn. Reson.* **2007**, *186*, 150−155.
(13) Bhattacharya, P.; Chekmenev, E. Y.; Reynolds, W. F.; Wagner, S.; Zacharias, N.; Chan, H. R.; Bünger, R.; Ross, B. D. Parahydrogen-Induced Polarization (PHIP) Hyperpolarized MR Receptor Imaging in Vivo: A Pilot Study of ^{13}C Imaging of Atheroma in Mice. *NMR Biomed.* **2011**, *24*, 1023−1028.
(14) Zacharias, N. M.; Chan, H. R.; Sailasuta, N.; Ross, B. D.; Bhattacharya, P. Real-Time Molecular Imaging of Tricarboxylic Acid Cycle Metabolism in Vivo by Hyperpolarized 1-C-13 Diethyl Succinate. *J. Am. Chem. Soc.* **2012**, *134*, 934−943.
(15) Adams, R. W.; Aguilar, J. A.; Atkinson, K. D.; Cowley, M. J.; Elliott, P. I. P.; Duckett, S. B.; Green, G. G. R.; Khazal, I. G.; Lopez-Serrano, J.; Williamson, D. C. Reversible Interactions with Para-Hydrogen Enhance NMR Sensitivity by Polarization Transfer. *Science* **2009**, *323*, 1708−1711.
(16) Atkinson, K. D.; Cowley, M. J.; Elliott, P. I. P.; Duckett, S. B.; Green, G. G. R.; Lopez-Serrano, J.; Whitwood, A. C. Spontaneous Transfer of Parahydrogen Derived Spin Order to Pyridine at Low Magnetic Field. *J. Am. Chem. Soc.* **2009**, *131*, 13362−13368.
(17) Gloggler, S.; Muller, R.; Colell, J.; Emondts, M.; Dabrowski, M.; Blumich, B.; Appelt, S. Para-Hydrogen Induced Polarization of Amino Acids, Peptides and Deuterium-Hydrogen Gas. *Phys. Chem. Chem. Phys.* **2011**, *13*, 13759−13764.
(18) Zeng, H.; Xu, J.; Gillen, J.; McMahon, M. T.; Artemov, D.; Tyburn, J.-M.; Lohman, J. A. B.; Mewis, R. E.; Atkinson, K. D.; Green, G. G. R.; et al. Optimization of SABRE for Polarization of the Tuberculosis Drugs Pyrazinamide and Isoniazid. *J. Magn. Reson.* **2013**, *237*, 73−78.
(19) Hövener, J.-B.; Schwaderlapp, N.; Borowiak, R.; Lickert, T.; Duckett, S. B.; Mewis, R. E.; Adams, R. W.; Burns, M. J.; Highton, L. A. R.; Green, G. G. R.; et al. Toward Biocompatible Nuclear Hyperpolarization Using Signal Amplification by Reversible Exchange: Quantitative in Situ Spectroscopy and High-Field Imaging. *Anal. Chem.* **2014**, *86*, 1767−1774.
(20) Shi, F.; Coffey, A. M.; Waddell, K. W.; Chekmenev, E. Y.; Goodson, B. M. Heterogeneous Solution NMR Signal Amplification by Reversible Exchange. *Angew. Chem., Int. Ed.* **2014**, *53*, 7495−7498.
(21) He, P.; Best, Q. A.; Groome, K. A.; Coffey, A. M.; Truong, M. L.; Waddell, K. W.; Chekmenev, E. Y.; Goodson, B. M. A Water-Soluble SABRE Catalyst for NMR/MRI Enhancement. Presented at the 55th ENC Conference, March 23−28, Boston, MA, 2014.
(22) Zeng, H.; Xu, J.; McMahon, M. T.; Lohman, J. A. B.; van Zijl, P. C. M. Achieving 1% NMR Polarization in Water in Less Than 1 min Using SABRE. *J. Magn. Reson.* **2014**, *246*, 119−121.
(23) Dechent, J. F.; Highton, L. A. R.; Green, G. G. R.; Duckett, S. B.; Spiess, H. W.; Schreiber, L. M.; Münnemann, K. Continuous Proton Hyperpolarization Via SABRE and Hollow Fibre Membranes. *Proc. Int. Soc. Mag. Reson. Med.* **2013**, 1937.
(24) Mewis, R. E.; Atkinson, K. D.; Cowley, M. J.; Duckett, S. B.; Green, G. G. R.; Green, R. A.; Highton, L. A. R.; Kilgour, D.; Lloyd, L. S.; Lohman, J. A. B.; et al. Probing Signal Amplification by Reversible Exchange Using an NMR Flow System. *Magn. Reson. Chem.* **2014**, *52*, 358−369.
(25) Mugler, J. P.; Altes, T. A. Hyperpolarized ^{129}Xe MRI of the Human Lung. *J. Magn. Reson. Imaging* **2013**, *37*, 313−331.
(26) Nelson, S. J.; Kurhanewicz, J.; Vigneron, D. B.; Larson, P. E. Z.; Harzstark, A. L.; Ferrone, M.; van Criekinge, M.; Chang, J. W.; Bok, R.; Park, I.; et al. Metabolic Imaging of Patients with Prostate Cancer Using Hyperpolarized 1-C-13 Pyruvate. *Sci. Transl. Med.* **2013**, *5*, 198ra108.
(27) Nikolaou, P.; Goodson, B. M.; Chekmenev, E. Y. NMR Hyperpolarization Techniques for Biomedicine. *Chem.—Eur. J.* **2014**, DOI: 10.1002/chem.201405253.
(28) Barskiy, D. A.; Kovtunov, K. V.; Koptyug, I. V.; He, P.; Groome, K. A.; Best, Q. A.; Shi, F.; Goodson, B. M.; Shchepin, R. V.; Coffey, A. M.; et al. The Feasibility of Formation and Kinetics of NMR Signal Amplification by Reversible Exchange (SABRE) at High Magnetic Field (9.4 T). *J. Am. Chem. Soc.* **2014**, *136*, 3322−3325.
(29) Cowley, M. J.; Adams, R. W.; Atkinson, K. D.; Cockett, M. C. R.; Duckett, S. B.; Green, G. G. R.; Lohman, J. A. B.; Kerssebaum, R.; Kilgour, D.; Mewis, R. E. Iridium N-Heterocyclic Carbene Complexes as Efficient Catalysts for Magnetization Transfer from Para-Hydrogen. *J. Am. Chem. Soc.* **2011**, *133*, 6134−6137.
(30) Vazquez-Serrano, L. D.; Owens, B. T.; Buriak, J. M. The Search for New Hydrogenation Catalyst Motifs Based on N-Heterocyclic Carbene Ligands. *Inorg. Chim. Acta* **2006**, *359*, 2786−2797.
(31) Torres, O.; Martin, M.; Sola, E. Labile N-Heterocyclic Carbene Complexes of Iridium. *Organometallics* **2009**, *28*, 863−870.
(32) Feng, B.; Coffey, A. M.; Colon, R. D.; Chekmenev, E. Y.; Waddell, K. W. A Pulsed Injection Parahydrogen Generator and Techniques for Quantifying Enrichment. *J. Magn. Reson.* **2012**, *214*, 258−262.
(33) Bowers, C. R.; Weitekamp, D. P. Para-Hydrogen and Synthesis Allow Dramatically Enhanced Nuclear Alignment. *J. Am. Chem. Soc.* **1987**, *109*, 5541−5542.
(34) Green, R. A.; Adams, R. W.; Duckett, S. B.; Mewis, R. E.; Williamson, D. C.; Green, G. G. R. The Theory and Practice of Hyperpolarization in Magnetic Resonance Using Parahydrogen. *Prog. Nucl. Magn. Res. Spectrosc.* **2012**, *67*, 1−48.
(35) Theis, T.; Truong, M.; Coffey, A. M.; Chekmenev, E. Y.; Warren, W. S. LIGHT-SABRE Enables Efficient in-Magnet Catalytic Hyperpolarization. *J. Magn. Reson.* **2014**, *248*, 23−26.
(36) Pravdivtsev, A. N.; Yurkovskaya, A. V.; Vieth, H.-M.; Ivanov, K. L. Spin Mixing at Level Anti-Crossings in the Rotating Frame Makes High-Field SABRE Feasible. *Phys. Chem. Chem. Phys.* **2014**, DOI: 10.1039/C4CP03765K.
(37) Crabtree, R. Iridium Compounds in Catalysis. *Acc. Chem. Res.* **1979**, *12*, 331−338.

(38) Tang, C. Y.; Lednik, J.; Vidovic, D.; Thompson, A. L.; Aldridge, S. Responses to Unsaturation in Iridium Mono(N-Heterocyclic Carbene) Complexes: Synthesis and Oligomerization of LIr(H)(2) Cl and LIr(H)(2) (+). *Chem. Commun.* **2011**, *47*, 2523−2525.
(39) Permin, A. B.; Eisenberg, R. One-Hydrogen Polarization in Hydroformylation Promoted by Platinum-Tin and Iridium Carbonyl Complexes: A New Type of Parahydrogen-Induced Effect. *J. Am. Chem. Soc.* **2002**, *124*, 12406−12407.
(40) van Weerdenburg, B. J. A.; Gloggler, S.; Eshuis, N.; Engwerda, A. H. J.; Smits, J. M. M.; de Gelder, R.; Appelt, S.; Wymenga, S. S.; Tessari, M.; Feiters, M. C.; et al. Ligand Effects of NHC-Iridium Catalysts for Signal Amplification by Reversible Exchange (SABRE). *Chem. Commun.* **2013**, *49*, 7388−7390.
(41) Song, Y. Q. Spin Polarization-Induced Nuclear Overhauser Effect: An Application of Spin-Polarized Xenon and Helium. *Concept Magn. Reson.* **2000**, *12*, 6−20.
(42) Navon, G.; Song, Y. Q.; Room, T.; Appelt, S.; Taylor, R. E.; Pines, A. Enhancement of Solution NMR and MRI with Laser-Polarized Xenon. *Science* **1996**, *271*, 1848−1851.
(43) Herskowitz, M.; Wisniak, J.; Skladman, L. Hydrogen Solubility in Organic Liquids. *J. Chem. Eng. Data* **1983**, *28*, 164−166.
(44) Brunner, E. Solubility of Hydrogen in 10 Organic-Solvents at 298.15-K, 323.15-K, and 373.15-K. *J. Chem. Eng. Data* **1985**, *30*, 269−273.
(45) Purwanto; Deshpande, R. M.; Chaudhari, R. V.; Delmas, H. Solubility of Hydrogen, Carbon Monoxide, and 1-Octene in Various Solvents and Solvent Mixtures. *J. Chem. Eng. Data* **1996**, *41*, 1414−1417.
(46) Adams, R. W.; Duckett, S. B.; Green, R. A.; Williamson, D. C.; Green, G. G. R. A Theoretical Basis for Spontaneous Polarization Transfer in Non-Hydrogenative Parahydrogen-Induced Polarization. *J. Chem. Phys.* **2009**, *131*, 194505.
(47) Hövener, J.-B.; Chekmenev, E.; Harris, K.; Perman, W.; Robertson, L.; Ross, B.; Bhattacharya, P. PASADENA Hyperpolarization of ^{13}C Biomolecules: Equipment Design and Installation. *Magn. Reson. Mater. Phys.* **2009**, *22*, 111−121.
(48) Waddell, K. W.; Coffey, A. M.; Chekmenev, E. Y. In Situ Detection of PHIP at 48 mT: Demonstration Using a Centrally Controlled Polarizer. *J. Am. Chem. Soc.* **2011**, *133*, 97−101.
(49) Roth, M.; Kindervater, P.; Raich, H.-P.; Bargon, J.; Spiess, H. W.; Muennemann, K. Continuous H-1 and C-13 Signal Enhancement in NMR Spectroscopy and MRI Using Parahydrogen and Hollow-Fiber Membranes. *Angew. Chem., Int. Ed.* **2010**, *49*, 8358−8362.